New Phytologist

A noncoding RNA transcribed from the *AGAMOUS* (*AG*) second intron binds to CURLY LEAF and represses *AG* expression in leaves

Hui-Wen Wu[1,2], Shulin Deng[1,2], Haiying Xu[2], Hui-Zhu Mao[2], Jun Liu[1], Qi-Wen Niu[1], Huan Wang[1] and Nam-Hai Chua[1,2]

[1]Laboratory of Plant Molecular Biology, Rockefeller University, New York, NY 10065-6399, USA; [2]Temasek Life Sciences Laboratory, Singapore City 117604, Singapore

Author for correspondence:
Nam-Hai Chua
Tel: +1 2123278126
Email: chua@mail.rockefeller.edu

Received: *7 February 2018*
Accepted: *23 April 2018*

New Phytologist (2018) **219:** 1480–1491
doi: 10.1111/nph.15231

Key words: *AGAMOUS (AG)*, CURLY LEAF (CLF), H3K27me3, intronic noncoding RNA (incRNA), second intron.

Summary

- Dispersed H3K27 trimethylation (H3K27me3) of the *AGAMOUS* (*AG*) genomic locus is mediated by CURLY LEAF (CLF), a component of the Polycomb Repressive Complex (PRC) 2. Previous reports have shown that the *AG* second intron, which confers *AG* tissue-specific expression, harbors sequences targeted by several positive and negative regulators.
- Using RACE reverse transcription polymerase chain reaction, we found that the *AG* intron 2 encodes several noncoding RNAs. RNAi experiment showed that *incRNA4* is needed for CLF repressive activity. *AG-incRNA4* RNAi lines showed increased leaf *AG* mRNA levels associated with a decrease of H3K27me3 levels; these plants displayed *AG* overexpression phenotypes.
- Genetic and biochemical analyses demonstrated that the *AG-incRNA4* can associate with CLF to repress *AG* expression in leaf tissues through H3K27me3-mediated repression and to autoregulate its own expression level.
- The mechanism of *AG-incRNA4*-mediated repression may be relevant to investigations on tissue-specific expression of Arabidopsis *MADS*-box genes.

Introduction

AGAMOUS (*AG*) is a MADS-box gene involved in the specification of stamens and carpels in flowers of wild-type (WT) *Arabidopsis thaliana*. *AG* expression is repressed by *APETALA1* (Riechmann *et al.*, 1996), *APETALA2 (*Drews *et al.*, 1991) and *CURLY LEAF* (*CLF*) (Schubert *et al.*, 2006), but activated by *LEAFY* (Busch *et al.*, 1999) and *WUSCHEL* (*WUS*) (Lohmann *et al.*, 2001). DNA sequences required for *AG* tissue-specific expression have been investigated. The *AG* native promoter itself is insufficient to confer tissue-specificity and enhancer sequences in intron 2 are required to repress expression in seedlings (Sieburth & Meyerowitz, 1997; Deyholos & Sieburth, 2000; Singer *et al.*, 2010). The mechanism of action of this intronic sequence is unknown.

In both animals and plants, Polycomb Repressive Complex 2 (PRC2) plays critical roles in tissue-specific gene expression by mediating H3K27 trimethylation (H3K27me3) to form repressive chromatin, thereby silencing gene expression (Whitcomb *et al.*, 2007; Molitor & Shen, 2013). H3K27me3 is catalyzed by a histone methyltransferase, and in Arabidopsis PRC2, CLF is the major H3K27 methyltransferase with SWINGER (SWN) sharing partial redundant function (Chanvivattana *et al.*, 2004). The repressive H3K27me3 marks left by PRC2 are then recognized by PRC1 which mono-ubiquitinates histone H2A (H2Aub) (Schatlowski *et al.*, 2008; Molitor & Shen, 2013). It is thought that CLF may form a PRC2-like complex named CLF-PRC2 to repress *AG* expression in vegetative tissues. Consistent with this view, the *AG* genomic locus carries dispersed H3K27me3 throughout leaf development (Schubert *et al.*, 2006).

On the one hand, Arabidopsis PRC2 may be targeted to genomic sites directly or indirectly. *LEAFY COTYLEDON2* (*LEC2*) promoter contains a putative polycomb response element (PRE), which might directly bind PRC2 (Berger *et al.*, 2011). On the other, PRC2 may be attracted to its target sites via interaction with other DNA-binding proteins. For example, *AG* can bind to the CArG boxes of the *WUS* locus to recruit PRC2 (Liu *et al.*, 2011) and AS1-AS2 heterodimer facilitates PRC2 binding to *BP* and *KNAT2* (Lodha *et al.*, 2013). Noncoding (nc) RNA may also facilitate PRC2 binding to target sites. *COLDAIR*, an Arabidopsis intronic ncRNA, has been shown to recruit PRC2 to repress the *FLOWER LOCUS C* (*FLC*) after vernalization (Heo & Sung, 2011).

During the last decade, high-throughput sequencing and computational analysis have identified thousands of long ncRNAs (lncRNAs) from plants; (Liu *et al.*, 2012; Wang *et al.*, 2014a, 2015). LncRNAs can be classified into three major groups: long intergenic ncRNA (lincRNA), intronic ncRNA (incRNA) and natural antisense transcripts (NATs) (Liu *et al.*, 2015). Several plant lncRNAs have been shown to regulate important biological processes: *COLDAIR* and *COOLAIR* specify flowering time by regulating the *FLC* locus (Liu *et al.*, 2010; Heo & Sung, 2011; Sun *et al.*, 2013), *LONG DAY-SPECIFIC MALE-FERTILITY-*

© 2018 The Authors
New Phytologist © 2018 New Phytologist Trust

ASSOCIATED RNA (*LDMAR*) controls rice fertility (Ding *et al.*, 2012), *HIDDEN TREASURE 1* (*HID1*) is involved in photomorphogenesis by regulating *PHYTOCHROME-INTERACTI NG FACTOR 3* (*PIF3*) (Wang *et al.*, 2014b), eTM-type lncRNA *IPS1* acts as a miR399 target mimic in phosphate homeostasis (Franco-Zorrilla *et al.*, 2007), ASCO lncRNA mediates alternative splicing by recruiting related regulators (Bardou *et al.*, 2014) and *AUXIN REGULATED PROMOTER LOOP* (*APOLO*) regulates polar auxin transport by controlling chromatin loop dynamics (Ariel *et al.*, 2014). An additional lncRNA, *COLDWRAP* has been recently identified from the repressed *FLC* promoter during vernalization (Kim & Sung, 2017). This lncRNA is involved in the formation of a repressive chromatin loop critical for maintaining the polycomb-medicated silencing of *FLC*. An ELF-induced lncRNA, *ELENA1*, directly interacts with Mediator 19a (MED19a) to activate plant innate immunity response (Seo *et al.*, 2017). *CDF5 LONG NONCODING RNA* (*FLORE*), a circadian-regulated lncRNA that is NATs of *CDF5* has been reported that links the circadian clock to photoperiodic flowering recently (Henriques *et al.*, 2017).

In order to examine the mechanism of *AG* repression in vegetative tissues of Arabidopsis, we have identified an incRNA, *AG-incRNA4*, from the *AG* intron 2. We showed that *AG-incRNA4* associated with CLF was required for the repressive activity of the latter. The absence of CLF or *AG-incRNA4* resulted in the derepression of *AG* and a reduction of H3K27me3 marks. *In vitro* and *in vivo* experiments provided evidence that *AG-incRNA4* may interact with CLF, thereby recruiting the CLF-PRC2 complex to repress *AG*. In addition, *AG-incRNA4* also recruited PRC2 to the *AG-incRNA4* promoter region to downregulate its own expression. Our results on the mechanism of *AG* repression may inspire future investigations on tissue-specific expression of other plant *MADS*-box genes and provide additional information on the role of lncRNAs in eukaryotes.

Materials and Methods

Generation of constructs

Various DNA fragments encoding potential intronic transcripts were cloned into *pH7GWIWG II* (Karimi *et al.*, 2002) to produce AGAMOUS (AG)-intronic noncoding (nc)RNA (incRNAi) constructs (Supporting Information Table S1). Sequence for *pAG-Intron 2:GUS* and deletion derivatives were synthesized (GenScript, Beijing, China) and then cloned into *pCAMBIA-1391Z* (Hajdukiewicz *et al.*, 1994). For *in vitro* and *in vivo* *AG-incRNAs*/CURLY LEAF (CLF interaction assays, DNA encoding the CLF CXC domain (Heo & Sung, 2011) was cloned into *pGEX-DC-3HA* to generate *pGEX-CLF^{cxc}-3HA* using LR clonase II (Invitrogen). The full length of CLF was placed downstream of its native promoter as *pCLF :CLF-FLAG* construct. For MS2-fusion RNA localization experiments, DNA fragments encoding *COLDAIR* (Heo & Sung, 2011), *RSM1* (Hamaguchi *et al.*, 2008), *AG-incRNA1* and *AG-incRNA4* were cloned into *pSCJ216-DC-MSCP-mcherry^{NLS}* (modified from *pSCJ216-DC* which is provided by Ulrich Z. Hammes) using LR clonase II (Invitrogen). Full-length *CLF* was cloned into *pBA-DC-GFP* using LR clonase II (Invitrogen) to generate *pBA-CLF-GFP*. A DNA fragment (300 bp) 5′ upstream of the *AG-incRNA4* transcription start site was considered as the putative promoter for the *incRNA4* and cloned into *pCAMBIA-1391Z* to generate *pAG-incRNA4:GUS*. All primers for PCR-based restriction and Gateway cloning are listed in Table S1.

RACE RT-PCR

RNAs were extracted from 2-wk-old seedlings of wild-type (WT; Col-0) and *clf*-28 (SALK_139371) (Method S1). Full-length ncRNAs were obtained using 5′ and 3′-end gene RACER (Invitrogen). We designed primer pairs for 5′ RACE reverse transcription polymerase chain reaction (RT-PCR) (Table S2). The 3′-end sequence of *AG-incRNA4* was identified by tilling PCR with specific primers (Table S2).

Plant materials and growth conditions

We transformed Arabidopsis WT plants by the floral dip method (Clough & Bent, 1998; Zhang *et al.*, 2006). The plant materials used are listed in Table S3. All Arabidopsis plants were grown at 20–22°C under a photoperiod, 16 h : 8 h, light : dark. Growth and phenotypes were analyzed using transgenic T_2 progeny plants.

AG-incRNAs silencing efficiency

The presence of *AG-incRNAs* (*RNA1, 2, 3* and *4*) in WT (Col-0) and different AG-incRNAi lines were determined by RT-PCR. A control without any reverse transcriptase (RT) was used to determine transcripts derived from the *AG* intronic region and *ACT2* level was used as an internal control. Silencing efficiencies of the various AG-incRNAi lines were assessed using primer sets 1, 2 and 3 to interrogate specific incRNAs (Table S2).

Detection of *AG* mRNA and *AG-incRNA4* levels

Total RNA (Method S1) from 2-wk-old seedlings and floral tissues of WT (Col-0) and *clf-28* were used for Northern blot hybridizations. To detect *AG-incRNA4*, ^{32}P-radiolabeled sense and anti-sense RNA probes (Table S4) were synthesized using MAXIscript® T7 Kit (Ambion). To determine *AG* mRNA levels, gene-specific ^{32}P-radiolabeled probes were synthesized by random priming (Agilent, Santa Clara, CA, USA) using the *AG* coding sequence as templates. *AG-incRNA4* and *AG* transcript levels were determined by RT-PCR.

Chromatin immunoprecipitation (ChIP) assay

Two-week-old seedlings of WT (Col-0) and AG-incRNAi lines grown on MS medium (Murashige & Skoog, 1962) were used. ChIP assays were performed (Bowler *et al.*, 2004), using antibodies recognizing H3K27me3 (Millipore), H3K36me3 (Abcam, Cambridge, MA, USA), H3K4me3 (Abcam) and monoclonal

© 2018 The Authors
New Phytologist © 2018 New Phytologist Trust

anti-FLAG M2® (Sigma). The primer pairs for chromatin modification, *AG* In2-21, 2-8, 2-3 and *AG* exon, and all primer pairs for CLF-targeted intron 2 regions, used are listed in Table S2.

In vitro RNA pull-down assay

Recombinant protein containing the CLF^{CXC} domain was purified from extracts of *Escherichia coli* (*E. coli*) carrying a *pGEX* expression system (GE Healthcare, Pittsburgh, PA, USA). Biotinylated RNAs (Table S4) were synthesized by MAXIscript® T7 Kit (Ambion). *In vitro* RNA pull-down assays were performed as described (Heo & Sung, 2011). The biotinylated-RNA bound proteins were detected by Western blots using an anti-GST monoclonal antibody (Santa Cruz Biotechnology, Dallas, TX, USA).

In vivo immunoprecipitation for CLF/*AG-incRNA4* interaction

CLF/*AG-incRNA4* association was assayed using nuclear extracts of 2-wk-old seedlings of *pCLF:CLF-FLAG/clf-28* and *pCLF:GFP-FLAG/clf-28*. Anti-FLAG M2® monoclonal antibody (Sigma) were used for immunoprecipitation. RNA extracted from the eluted immunoprecipitated-complex described in Method S1. RT-PCR was used to detect *AG-incRNA4* using appropriate primer sets (Table S2).

Co-localization of CLF and *AG-incRNAs* in *Nicotiana benthamiana*

Agrobacterium tumefaciens EH105 cell harboring DNA sequences for *AG-incRNAs*, MSCP-$mCherry^{NLS}$ and *pBA-CLF-GFP* (Table S1) were premixed before being infiltrated into *N. benthamiana* leaves. Confocal microscopy was performed 2 d after infiltration using an Inverted LSM 780 laser scanning confocal microscope (Zeiss). Excitation and emission were at: 488 and 500–530 nm, for GFP; and 543 and 585–615 nm, for mCherry.

GUS staining

β-Glucuronidase (GUS) activity of *pAG:AGincRNAs-35SminiGUS* transgenic lines were analyzed by staining (Senecoff *et al.*, 1996). Two transgenic lines of each construct (Table S3) from 2-wk-old seedlings and flower tissues were collected for GUS activity assays. To examine *pAG-incRNA4:GUS* expression in the *clf*-28 background, we crossed *pAG-incRNA4:GUS* transgenic lines (#2, #3 and #4) with the *clf-28* mutant. Eight seedlings of transgenic T_2 progenies were used for GUS staining and mRNA levels were determined by quantitative PCR (qPCR).

Results

AG intron 2 encodes several ncRNAs

In order to explore possible epigenetic regulation of the *AG* locus, we reanalyzed our previously published strand-specific RNA-seq datasets (Liu *et al.*, 2012) and detected several RNA fragments on the forward strand of *AG* intron 2 suggesting putative intronic ncRNAs. Using RLM RACE PCR, we identified in *clf-28* seedlings four *AG-incRNAs*, designated *AG-incRNA1*, *2*, *3* and *4* (Fig. S1a). The presence of several poly A repeats within intron 2 precluded identification of the *AG-incRNA4* 3′-end by 3′ RACE; therefore, we used specific primers instead (Fig. S1b). Figure S1a and b show that *AG-incRN4* was at least 999 nt long. To avoid genomic DNA contamination, RNAs without RT were interrogated by PCR as a control. *AG-incRNA4* transcript can be amplified from cDNA samples (Fig. S2) as a true RNA transcript from *AG* intron 2.

Phenotypes of AG-incRNAi transgenic lines

In order to investigate the putative function of the incRNAs, we generated RNAi transgenic lines directed against the various specific intron 2 regions. The effectiveness of the RNAi was assessed using specific primer sets (Fig. 1a) to determine *AG-incRNA* levels in WT and AG-incRNAi transgenic lines. Figure 1(a,b) show the silencing of *AG-incRNA1* in *AG-In2a #39* and the silencing of *AG-incRNA2/3* in *AG-In2c #41*. In *AG-In2c #41*, *AG-incRNA4* was still expressed as probed by primer set 3; *AG-incRNA4*, however, was not detectable in *AG-in2e #49*. This line (#49) displayed curly leaves in addition to having defective petals and sepals (Fig. 1c) with phenotypes similar to those of *clf-28* plants and transgenic Arabidopsis overexpressing *AG* (Mizukami & Ma, 1992). Similar phenotypes were obtained for another transgenic line *AG-incRNAi-In2d/e #65*. By contrast, *AG-incRNAi-In2a #39*, which did not express *AG-incRNA1*, and AG-incRNAi-In2c#41 plants, which had no detectable *AG-incRNA-2/3*, were like WT plants (Fig. 1c). *AG* transcript levels in *clf*-28, *AG-incRNAi-In2d/e* (line #26 & #65) and *AG-incRNAi-In2e* (line #49 & #6) accumulated up to 6.9–23-fold compared to WT control (Fig. 1d). Consistent with their WT phenotype, no apparent changes in *AG* transcript levels were seen in *AG-incRNAi-In2a* (line #39 & #40) and *AG-incRNAi-In2c* (line #41 & #44) transgenic seedlings (Fig. 1c).

We profiled accumulation of small (sm)RNAs in the *AG-incRNAi-In2e #49* line. SmRNAs were generated from both strands of sequences encoding *AG-incRNA4* and no smRNA was found targeting other neighboring regions of the *AG* locus (Fig. S3). SmRNAs were derived from the Intron 2e target sequence and also from other sequences encoding *AG-incRNA4* (Fig. S3), suggesting limited spreading of the silencing signal. These results suggested that the high accumulation of *AG* transcript in In-2de/e and In-2e lines (Fig. 1d) was likely due to the absence of *AG-incRNA4*.

The presence of 24 nt-smRNA raised the possibility that *AG* level might be changed by RNA-directed DNA methylation (RDdM) of *AG* intron 2 sequences (Shibuya *et al.*, 2009). To investigate this possibility, we crossed *AG-incRNAi-In2a #39*, *AG-incRNAi-In2c #41*, *AG-incRNAi-In2e #49* and *AG-incRNAi-In2d/e #65* with *ago4-2* (Agorio & Vera, 2007) to eliminate 24-nt mediated DNA methylation. The introduction of the *ago4-2* mutation had no significant impact on *AG* transcript levels (Fig. 1f) and *AG*-related morphological phenotype (Fig. 1e) of

© 2018 The Authors
New Phytologist © 2018 New Phytologist Trust

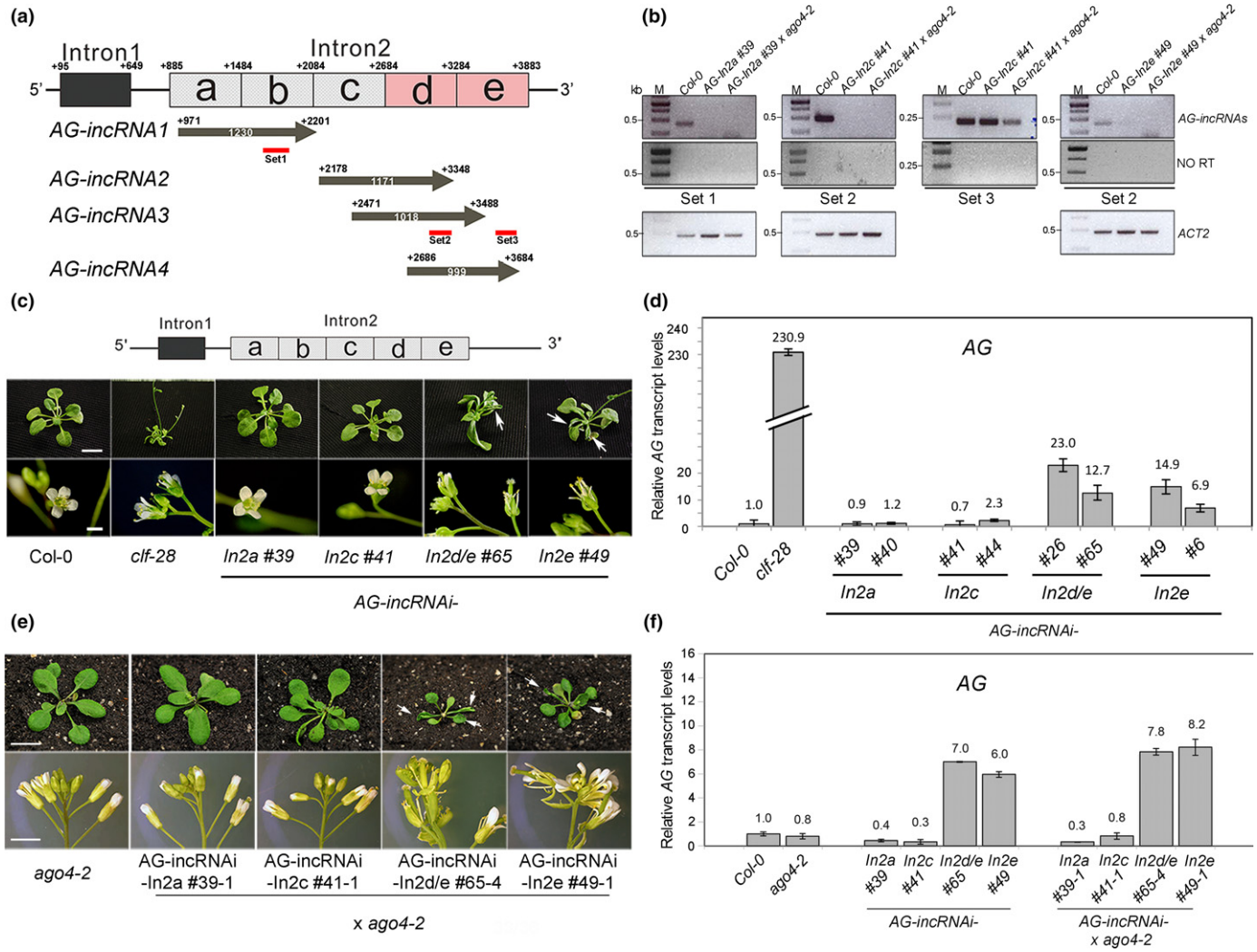

Fig. 1 *AGAMOUS* (*AG*)-*incRNA4* acts as a co-repressor of CURLY LEAF (CLF) for *AG* repression in vegetative tissues. (a) Schematic presentation of putative nonconding (nc)RNA transcript position and their primer set positions for confirming silencing efficiency within *AG* Intron 2. (b) Confirmation of silencing efficiency of *AG-incRNA* transcript using primer sets from Intron 2. The primer sets 1, 2 and 3 for silenced *AG-incRNAs* positions, and for *ACT2* (*ACT2_500*) are listed in Supporting Information Table S2. Reverse transcription polymerase chain reaction (RT-PCR) was used to detect transcripts of *AG-incRNAs* and no reverse transcriptase (RT) control was performed with 40 cycles, and reactions to detect *ACT2* were performed with 25 cycles. (c) Phenotypes of RNAi lines targeting different regions of *AG* Intron 2 and of *clf-28* mutant. Bars: 1.0 cm (upper panels); 0.1 cm (lower panels). (d) *AG* transcript levels in different RNAi lines and *clf-28* mutant. *AG* transcript levels (fold change; mean± SD of quantitative (q) RT-PCR; $n = 3$) were presented relative to wild-type (WT) levels which were set as 1. (e) Phenotypes of RNAi lines targeting different regions of *AG* Intron 2 in the *ago4-2* background. Bars: 1.0 cm (upper panels); 0.2 cm (lower panels). (f) *AG* transcript levels in different RNAi lines in the *ago4-2* background. *AG* transcript levels (fold change; mean± SD of qRT-PCR; $n = 3$) were presented relative to the WT levels which were set as 1. All experiments were performed with three independent biological replicates.

the AG-incRNAi lines. The total methylation levels of CGN, CHG and CHH (C = cytosine; G = guanine; N = any nucleotide; H = A, T or C) were compared in a CLF-targeted region of AG-Intron 2 (+2616 to +3348) (Fig. S4, upper panel) between AG-incRNAi lines and AG-incRNAi/*ago4-2* lines. As expected, DNA methylation of CGN, CHG and CHH of *AG-incRNAi-In2e #49* and *AG-incRNAi-In2d/e #65* were reduced under *ago4-2* background (Fig. S4) but there was no effect on *AG* de-repression in vegetative tissues (Fig. 1e,f).

RT-PCR experiments showed that the silencing of specific incRNAs was not affected by the *ago4-2* mutation (Fig. 1b). Taken together, our results suggest that *AG* overexpression phenotypes and the high *AG* transcript accumulation in AG-In2d/e and AG-In2e lines resulted from reduced levels of *AG-incRNA4* caused by post-transcriptional gene silencing (PTGS).

GUS expression in vegetative tissues of *pAG-Intron2:GUS* constructs

The loss-of-function experiments described above were complemented with gain-of-function experiments. *Cis*-elements for tissue-specific expression of *AG* were previously localized to intron 2 (Sieburth & Meyerowitz, 1997) and relocation of intron 2 to the 5′ upstream region of a minimal 35S

© 2018 The Authors
New Phytologist © 2018 New Phytologist Trust

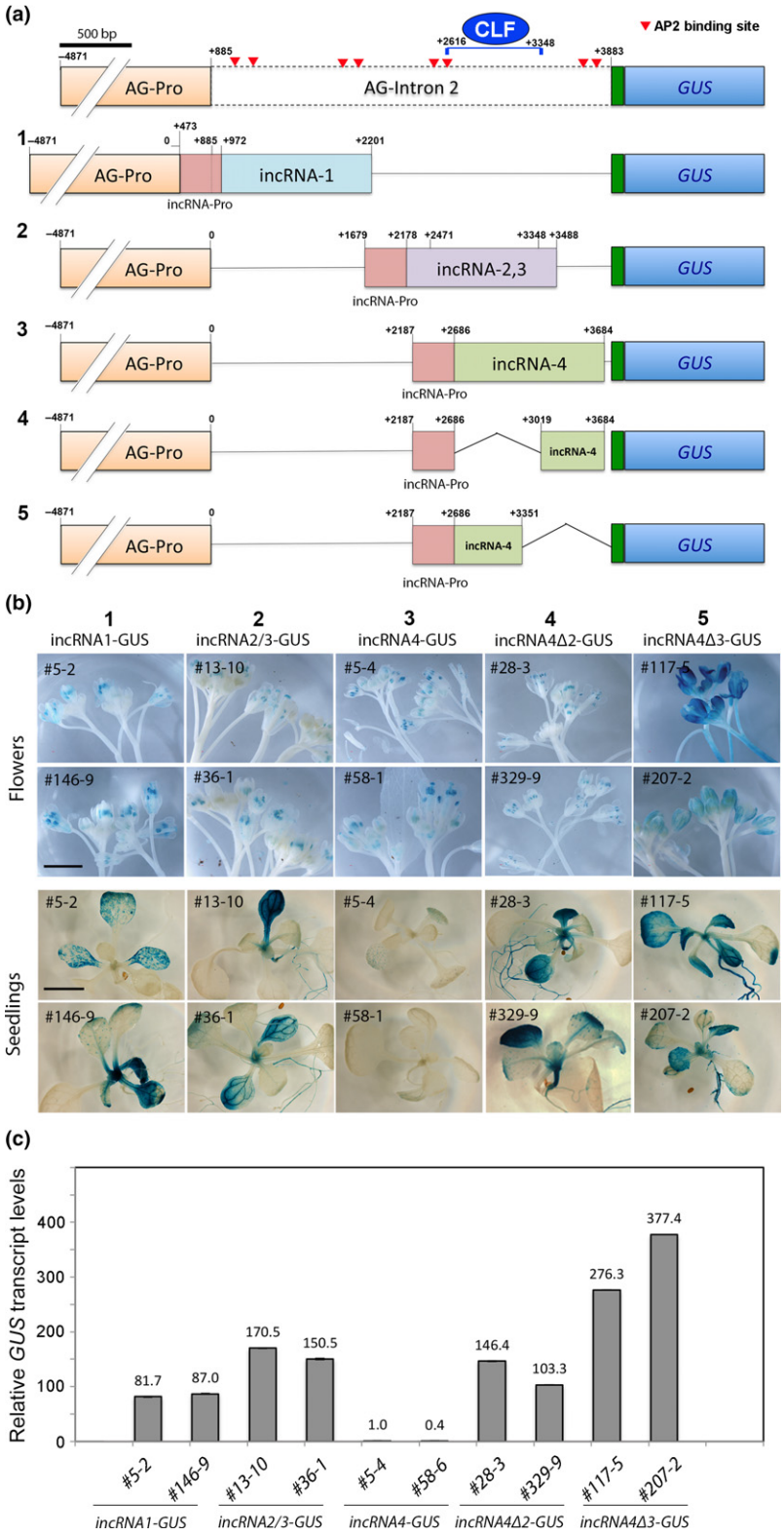

Fig. 2 Expression patterns of *pAG-Intron 2:GUS* and deletion derivatives. (a) All construct contains DNA sequences for the *AGAMOUS* (*AG*) promoter (pAG; −4871 to 0) and Intron 2 (top schematic diagram) or Intron 2 (its) deletion mutants that were placed upstream of a minimal 35S promoter (−60 to +9). In construct 1, the intronic sequences (contained) 413 bp from the 3′ end of Intron 1 and 88 bp from Intron 2 as *incRNA-1* promoter (+473 to +972) (inc, intronic noncoding). The construct also contained sequences encoding *incRNA-1* (+972 to +2201). Construct 2 contains sequences encoding *incRNA-2* (+2178 to +3348) and *incRNA-3* (+2471 to +3488). Construct 3 contains sequences encoding *incRNA-4* (+2686 to +3684). Constructs 4 and 5 were deletion mutants of construct 4. In all constructs, sequences encoding the various *incRNAs* were indicated along with CURLY LEAF (CLF) (Fig. 7) and AP2 binding sites. (b) β-Glucuronidase (GUS) expression patterns in flowers and seedlings of the various constructs. Bars: 0.3 cm (upper panel, flowers); 0.5 cm (lower panel, seedlings). (c) GUS transcript levels (fold-change; mean ± SD of quantitative reverse transcription polymerase chain reaction (qRT-PCR; $n = 3$) in seedlings of the various constructs. All experiments were performed with three independent biological replicates.

promoter conferred similar tissue-specificity on a *GUS* reporter gene with little or no expression in vegetative tissues (Deyholos & Sieburth, 2000). We used a similar *AG* promoter-Intron 2:GUS construct described by Deyholos & Sieburth (2000) to identify intron 2 sequences responsible for repression of GUS expression in vegetative tissues.

We tested three different DNA sequences derived from intron 2, encoding *incRNA1*, *incRNA2/3* and *incRNA4* (Fig. 2a). GUS

© 2018 The Authors
New Phytologist © 2018 New Phytologist Trust

expression was found in seedlings containing constructs 1, 2, 4 and 5 (Fig. 2b). Only construct 3 (Fig. 2a), which contained DNA sequences for *incRNA-4*, was able to confer tissue-specificity with little GUS expression in seedlings (Fig. 2b,c), suggesting *GUS* repression in vegetative tissues. However, release of *GUS* repression in seedlings was seen in two different deletion mutants of construct 3, which disrupted the coding sequences of *incRNA4* (Fig. 2). These results show that DNA sequence encoding full-length *incRNA4* is necessary and sufficient to confer repression of GUS expression in seedlings.

AG-incRNA4 and mRNA levels in seedlings and floral tissues

The *AG* locus in Arabidopsis WT plants is repressed by CLF-mediated dispersed H3K27me3 (Schubert *et al.*, 2006). To investigate the role of *AG-incRNA4* in CLF-mediated repression, we examined the expression of *AG-incRNAs* in WT seedlings and floral tissues. We found the sense *AG-incRNA4* slightly accumulated in seedlings of *clf*-28 compared to WT plants. This finding suggested that *AG-incRNA4* expression itself might be repressed by CLF (Fig. 3) and the repression was released in *clf*-28 seedlings. A similar result of higher intronic transcript levels was found in *clf-28* shoot (Fig. S1c) (Liu *et al.*, 2016).

Unfortunately, the very low expression levels of *AG-incRNA4* precluded its detection in WT seedlings. However, even at a very low expression level, *AG-incRNA4* might play a role in *AG* gene repression. We further investigated *AG-incRNA4* and *AG* mRNA levels in seedlings and floral tissues by RT-PCR. We found that *AG-incRNA4* levels were undetectable in WT but slightly increased in *clf-28* seedlings. For floral tissues, *AG-incRNA4* accumulated to a higher level in *clf*-28 compared to WT plants.

Chromatin immunoprecipitation (ChIP) assay

In order to investigate whether H3K27me3 methylation on the *AG* locus is triggered by *AG-incRNAs* and CLF, we performed ChIP in *clf*-28 and AG-incRNAi lines. H3K27me3 levels were much decreased within the region of *AG-incRNA4* (2-3 and 2-8) in *clf*-28, as well as *AG-incRNA4* RNAi lines (*AG-incRNAi-In2d/e #26*, *#65* and *AG-incRNAi-In2e #49*, *#6*) (Fig. 4). These results suggested that both CLF and *AG-incRNA4* act together to form H3K27me3 marks.

We also examined whether the *AG* locus is marked by H3K36me3 and H3K4me3. Figure 4 shows that the enrichment of H3K36me3 and H3K4me3 in different tested regions of WT were less than the corresponding regions in *clf-28*. However, there was no enrichment of H3K36me3 in transgenic lines of *AG-incRNAi-In2d/e* and *AG-incRNAi-In2e* (Fig. 4). Overall, our results did not show any significant difference between WT and AG-incRNAi lines with respect to H3K36me3 and H3K4me3 levels.

In vitro and *in vivo* pull-down assays for CLF/*AG-incRNA4* interaction

Based on the results of *COLDAIR* (Heo & Sung, 2011), we surmised that *AG-incRNA4* may directly bind to CLF. Therefore, we performed RNA pull-down assays using the GST tagged-CLF^{CXC} protein and biotin tagged-*AG-incRNA4* transcripts. *GFP* transcripts and *COLDAIR* transcripts were used as negative and positive controls, respectively. Figure 5(a) shows that CLF^{CXC} protein was pulled down directly by the sense strand of *AG-incRNA4* and *COLDAIR*, but not by antisense (AS) *AG-incRNA4* and *GFP*-biotin RNA. Surprisingly, *AG-incRNA1* was also pulled down by CLF. According to our result in Figs 1 and 5(a), *AG-incRNA1* may be bound to CLF but without any function in *AG* repression.

Next, we addressed possible *in vivo* interaction between CLF and *AG-incRNA4* by RNA immunoprecipitation. To avoid possible artifacts owing to overexpression, we generated CLF-FLAG complementation line under a *CLF* native promoter for *in vivo* RNA immunoprecipitation. As expected, the *AG-incRNA4* specifically bound to CLF-FLAG prepared from 2-wk-old

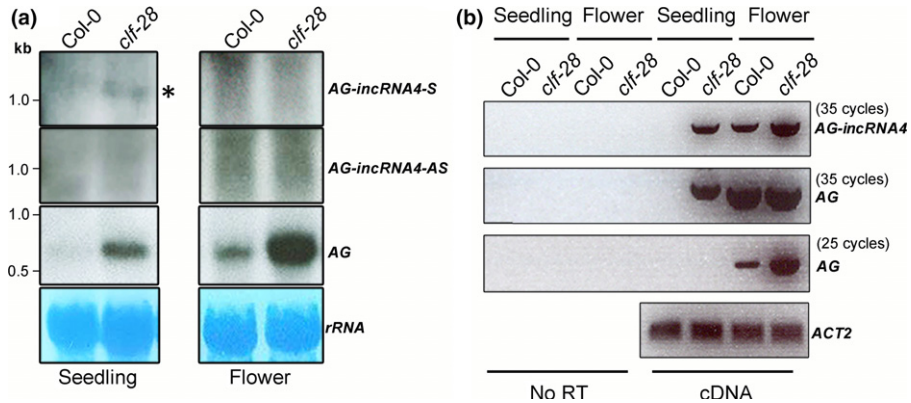

Fig. 3 Expression levels of *AGAMOUS* (*AG*) mRNA and its *incRNA4* in wild-type (WT) and in *clf*-28 (inc, intronic noncoding). (a) Detection of *AG-incRNA4* and *AG* mRNA by Northern blots. The detection of sense and antisense (AS) *AG-incRNA4* are shown on the top and the second panel. Asterisk (*) indicates sense *AG-incRNA4* in the top panel. 5S ribosomal RNA (*rRNA*) was used as a loading control. (b) Levels of *AG-incRNA4* and *AG* mRNA detected by reverse transcription polymerase chain reaction (RT-PCR). Specific primers were used to amplify *AG-incRNA4*, *AG* and *ACT2* transcripts (Supporting Information Table S2). RT control was used to determine transcripts from the *AG* intronic region.

© 2018 The Authors
New Phytologist © 2018 New Phytologist Trust

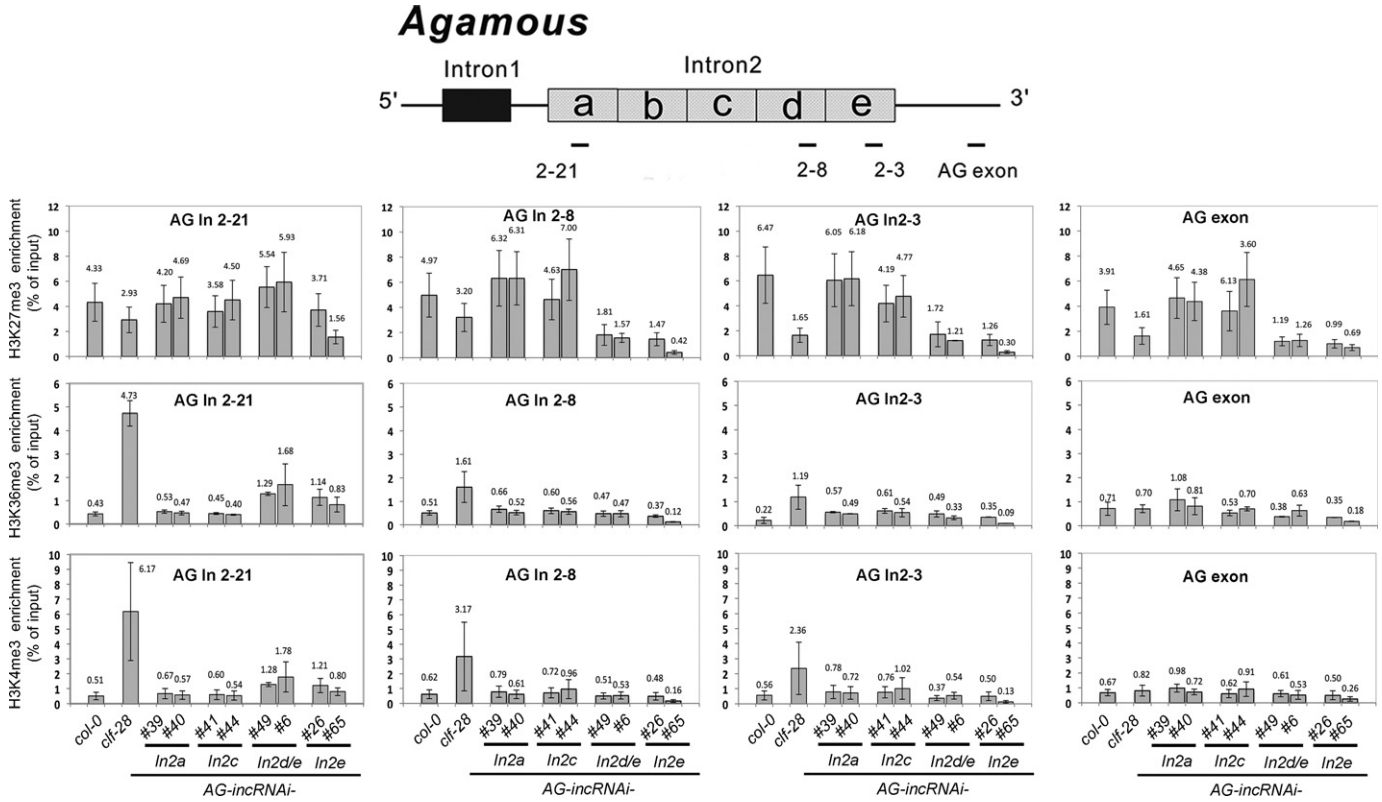

Fig. 4 Histone modifications associated with the *AGAMOUS* (*AG*) chromatin in wild-type (WT), *clf-28* and RNAi transgenic lines targeting different *AG* Intron 2 regions. The relative amounts of DNA in the input and immunoprecipitated (IP) samples were determined by real-time PCR, with three biological replicates for each sample. Enrichment was determined as the proportion of the input DNA recovered in the immunoprecipitated sample. Bars represent average values ± SD ($n = 3$ biological replicates). Numbers above the bars represent enrichment (% of input).

seedlings but no *AG-incRNA4* was pulled down in GFP-FLAG control line (Fig. 5b).

Subcellular co-localization of *AG-incRNA4* and CLF

In order to further investigate *in vivo* interaction between *AG-incRNA4* and CLF (Fig. 6a), we determined their subcellular localization in *N. bethamiana* by transient expression. Figure 6(b) shows that *AG-incRNA4* and *COLDAIR* co-localized with CLF and formed nuclear speckles. These results implied that *AG-incRNA*/CLF and *COLDAIR*/CLF might form complexes comprising proteins and RNAs from the surrounding nucleoplasm (Cheung & Reddy, 2012). By contrast, the nonfunctional *AG-incRNA1* showed similar result as *RSM1*, which served as a negative control (Fig. 6b).

AG-incRNA4 is needed for CLF docking on *AG* intron 2

We scanned the entire *AG* intron 2 for CLF binding sites by ChIP. Figure 7(a) shows a higher enrichment of CLF in genomic regions covering the *AG-incRNA4* promoter and the 5′-end of *AG-incRNA4* (*c.* +2616 to +3348 within *AG* intron 2). Hence, we checked this region in *AG-incRNAs* silenced lines and its control plants, such as *pCLF:CLF-FLAG/clf-28* × *Col-0*, *pCLF:CLF-FLAG/clf-28* × *AG-incRNAIn2a #39*, *pCLF:CLF-FLAG/clf-28* × *AG-incRNAIn2c #41*, *pCLF:CLF-FLAG/clf-28* × *AG-incRNAIn2d #65*, *pCLF:CLF-FLAG/clf-28* × *AG-incRNAIn2d/e #49* and its non-binding control, Col-0. Figure 7(b) shows that the CLF binding affinity on *AG* intron 2 was decreased in *pCLF:CLF-FLAG/clf-28* × *AG-incRNAIn2d #65* and *pCLF:CLF-FLAG/*

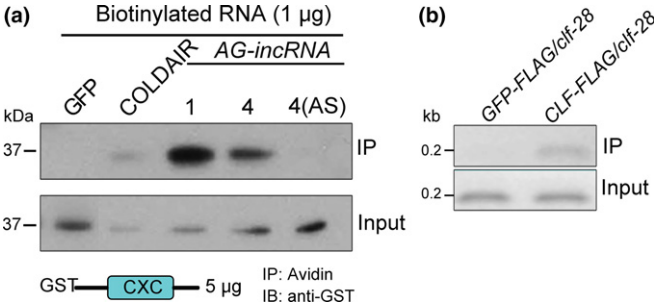

Fig. 5 *AGAMOUS* (*AG*)-*incRNA4* binds to CLF of Polycomb Repressive Complex 2 (PRC2) (inc, intronic noncoding). (a) *In vitro* pull-down of CLF^{CXC} protein by biotinylated *AG-incRNA4*. *AG-incRNA4* (AS) was an antisense of *AG-incRNA4*. *GFP* and *COLDAIR* transcripts were used as negative and positive controls, respectively. The CXC domain of CLF was used for *in vitro* binding assays. Monoclonal anti-GST was used for detection. (b) *In vivo* immunoprecipitation of CLF-FLAG fusion protein and *AG-incRNA4* in p*CLF:CLF-FLAG/clf*-28 complemented line. Monoclonal FLAG M2® was use for *in vivo* immunoprecipitation. The presence of *AG-incRNA4* was checked using reverse transcription polymerase chain reaction (RT-PCR) with specific primer pairs AG In2-7 (Supporting Information Table S2). All experiments were performed with three independent biological replicates.

© 2018 The Authors
New Phytologist © 2018 New Phytologist Trust

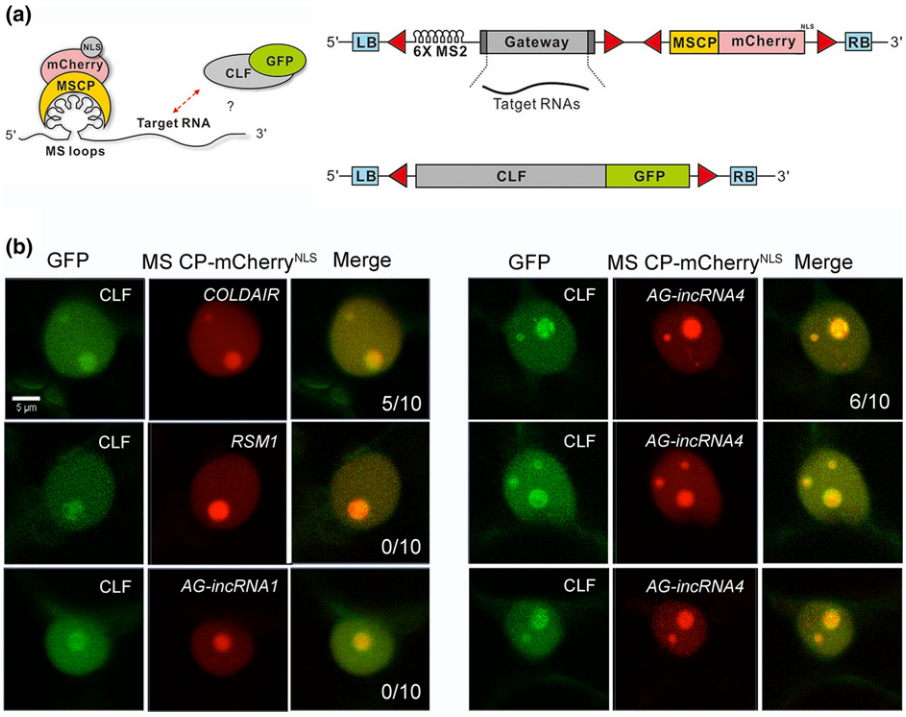

Fig. 6 Localization of CURLY LEAF (CLF) and *AGAMOUS* (*AG*)-*incRNA1* and *4* via Agrobacterial transient co-expression in *Nicotiana benthamiana* (inc, intronic noncoding). (a) Schematic representation of subcellular localization of 6 × MS2-Target RNAs and CLF-GFP (GFP, green fluorescent protein). (b) Transient co-expression of CLF-GFP and 6xMS-*AG-incRNA1* and *4* fusion RNAs detected by the MS CP-mCherry^{NLS} fusion protein. An enlarged image of the nucleus was shown in each panel to analyze co-localization of CLF and RNAs. *COLDAIR* and *RSM1* mRNA served as positive and negative control, respectively. Bar, 5 μm. The ratio in each panel indicates the number of nuclei with speckles among the total number of analyzed cells. The right panel shows different nuclei speckles from six of the total 10 CLF and *AG-incRNA4* co-expressing cells.

clf-28 × *AG-incRNAIn2d/e #49* crossed lines which were silenced with respect to *AG-incRNA4*. This result suggests that *AG-incRNA4* is needed for CLF binding to *AG* intron 2.

Tissue-specific *GUS* expression control by *AG* incRNA promoter

In order to see if the tissue-specific expression pattern of *AG-incRNA4* is controlled by the ncRNA promoter itself, we scanned for putative *AG-incRNA4* promoter regions within the *AG* second intron. Figure 8(a) shows that a 300-bp DNA fragment upstream of the 5′-end of the *AG-incRNA4* start site was sufficient to activate GUS expression in 2-wk-old and 3-wk-old seedlings (Fig. 8b). The GUS expression levels varied depending on the developmental stages of *pAG-incRNA4:GUS* lines. *GUS* mRNA levels in four independent lines showed higher expression levels in 2-wk-old seedlings but the expression levels decreased subsequently (Fig. 8c).

We hypothesized that *AG-incRNA4* might be downregulated by CLF because of the high *AG-incRNA4* expression levels in *clf-28* leaf tissues (Fig. S1c, 3). To test this hypothesis, *pAG-incRNA4:GUS* lines were introduced into the *clf-28* background and *GUS* mRNA levels were examined by qPCR. *GUS* mRNA levels increased to 6.9-fold and 62-fold in 3-wk-old and 4-wk-old seedlings of *pAG-incRNA4:GUS #3/clf-28* line compared to *pAG-incRNA4:GUS #3/WT* line (Fig. 8d, middle panel). Similar results were obtained in *pAG-incRNA4:GUS #2/clf-28* and *pAG-incRNA4:GUS #4/clf-28* lines compared to WT control (Fig. 8d). We found that *pAG-incRNA4:GUS* was only expressed in the cotyledons in 3-wk-old seedlings of *pAG-incRNA4:GUS #3/WT* (Fig. 8e, upper left panel). By contrast, GUS expression was detected in all true leaves of *pAG-incRNA4:GUS #3/clf-28* plants (Fig. 8e, upper right panel); moreover, its expression was higher than that in *pAG-incRNA4:GUS #3/WT*. GUS expression was almost undetectable in 4-wk-old seedlings of *pAG-incRNA4:GUS #3/WT*, whereas it was still detected in true leaves and cotyledons of 4-wk-old seedling of *pAG-incRNA4:GUS #3/clf-28* (Fig. 8e, lower panel).

Discussion

Long, noncoding (lnc)RNAs are known to play important regulatory roles in the developmental processes and stress responses of eukaryotes (Karapetyan *et al.*, 2013). Although the functions of plant lncRNAs are just beginning to be characterized, available evidence shows that they may regulate similar molecular processes as in other eukaryotes (Yamada, 2017). Here, we have identified four intronic ncRNAs from *AGAMOUS* (*AG*) intron 2 and provided evidence that *AG-incRNA4* acts as a co-repressor with CURLY LEAF (CLF) to confer *AG* tissue-specific expression.

AG-incRNA4 required to repress *AG* expression

Using reverse transcription polymerase chain reaction (RT-PCR) we identified four incRNAs from *AG* intron 2, which varied in length from 1000 to 1200 nt. These transcripts were confirmed to be 5′-capped by RLM-RACE PCR (Ambion) and further Northern blot analysis identified *AG-incRNA4* as a positive sense RNA (Fig. 3a). Using RNAi to knock-down expression of incRNAs, we provided preliminary evidence that among the four incRNAs only *AG-incRNA4* plays a role in repressing *AG* expression in leaves. In *AG-incRNAi-In2e* transgenic plants, silencing of *AG-incRNA4* led to *AG* expression in seedlings. Although the expressed dsRNA targeted only a portion of the *AG-incRNA4* (Fig. S3), smRNAs were

© 2018 The Authors
New Phytologist © 2018 New Phytologist Trust

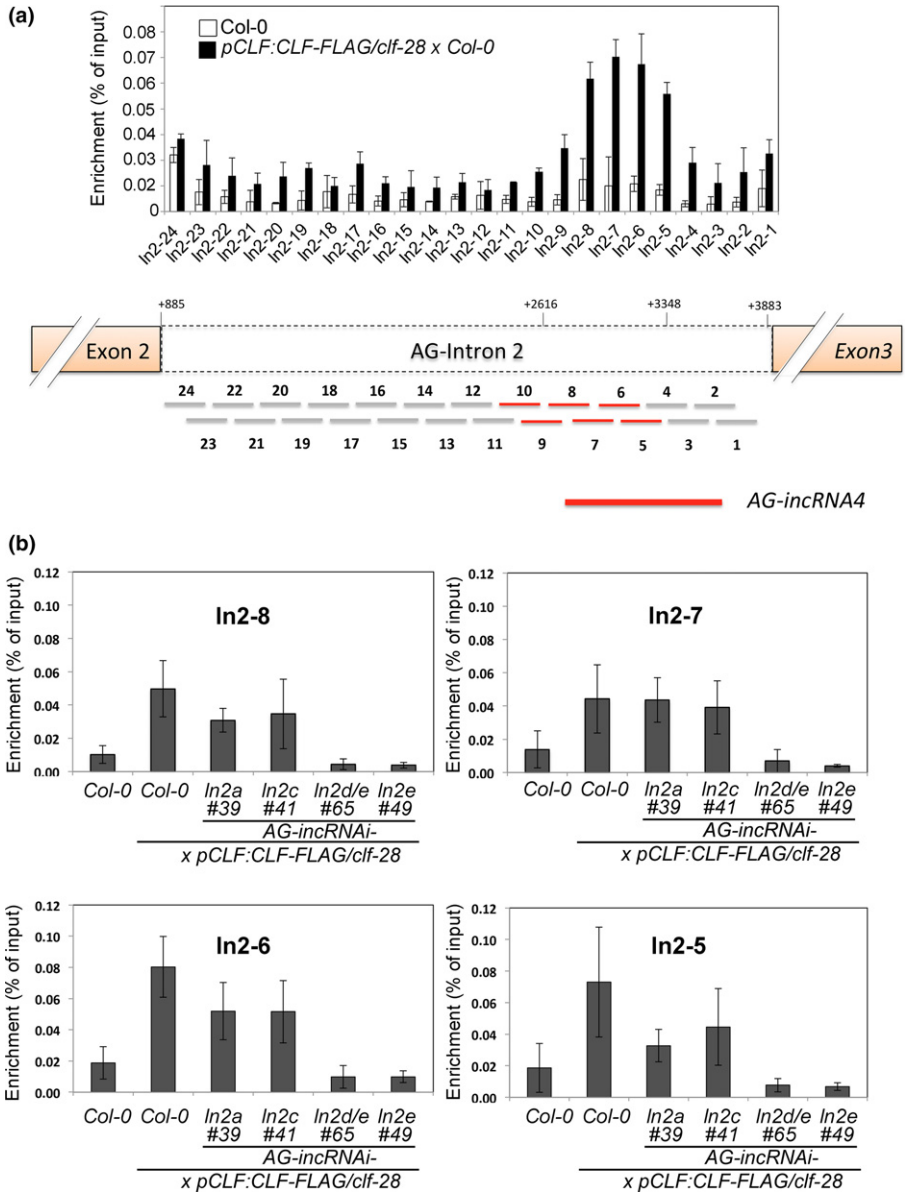

Fig. 7 Binding of CURLY LEAF (CLF)-FLAG to *AGAMOUS* (*AG*) Intron 2 in wild-type (WT) and in various AG-incRNAi lines (inc, intronic noncoding). (a) Characterization of CLF binding region on *AG* Intron 2. (b) Reduced level of CLF-FLAG on *AG* Intron 2 in AG-incRNAi lines. T_2 progenies of *pCLF:CLF-FLAG/clf-28* complementary line crossed with various AG-incRNAi lines or WT (as positive control), and monoclonal FLAG M2® were used for ChIP analysis. Enrichment was determined as the proportion of the input DNA that was recovered in the immunoprecipitated sample (mean ± SD of ChIP-PCR; $n = 3$). All experiments were performed with three independent biological replicates.

generated from the full-length *AG-incRNA4*. This loss-of-function experiment was complemented by gain-of-function experiments. As a reference construct, we used *pAG-I::GUS*, which contains intron 2 relocated to the 5′ region of the transcription start site but downstream of the *AG* native promoter and a *β-Glucuronidase* (*GUS*) coding sequence as a reporter (Deyholos & Sieburth, 2000). GUS expression in seedlings was repressed by sequences encoding *incRNA-4* but not by those encoding *incRNA1* or *incRNA2/3*. Deletion of the full-length sequence for *incRNA4* abrogated the repression and allowed GUS expression. Taken together, our results showed that *AG-incRNA4* is needed to repress *AG* expression in vegetative tissues.

AG-incRNA4 acts as a co-repressor of CLF

CLF is expressed ubiquitously and it controls leaf and flower morphology as well as flowering time (Goodrich *et al.*, 1997). *AG*, a target of CLF, carries an epigenetic feature of dispersed H3K27me3 and localized H3K27me2 (Schubert *et al.*, 2006). In *clf-28*, H3K27me3 levels in the *AG* locus were decreased along with de-repression of *AG* (Fig. 4). Because similar results were obtained in *AG-incRNA4* RNAi lines (Fig. 4), we hypothesized that *AG-incRNA4* might work as a co-repressor of CLF. This hypothesis was bolstered by the observation that *AG-incRNA4* interacts with CLF *in vitro*. Moreover, *AG-incRNA4* also associates with CLF *in vivo* and the ncRNA/CLF complex appears to be sequestered as nuclear speckles (Fig. 6b).

By ChIP assay (Fig. 7a), we found that CLF binds to a position (*c.* +2616 to +3348 within *AG* intron 2) covering the *AG-incRNA4* promoter and the 5′-end of *AG-incRNA4*. However, the binding affinity of CLF-FLAG to *AG* intron 2 was decreased in *AG-incRNA4* knockdown lines, but not in *AG-incRNA1 or AG-incRNA2/3* knockdown controls. These results suggest that *AG-incRN4* is needed for CLF binding onto its target site in *AG*

© 2018 The Authors
New Phytologist © 2018 New Phytologist Trust

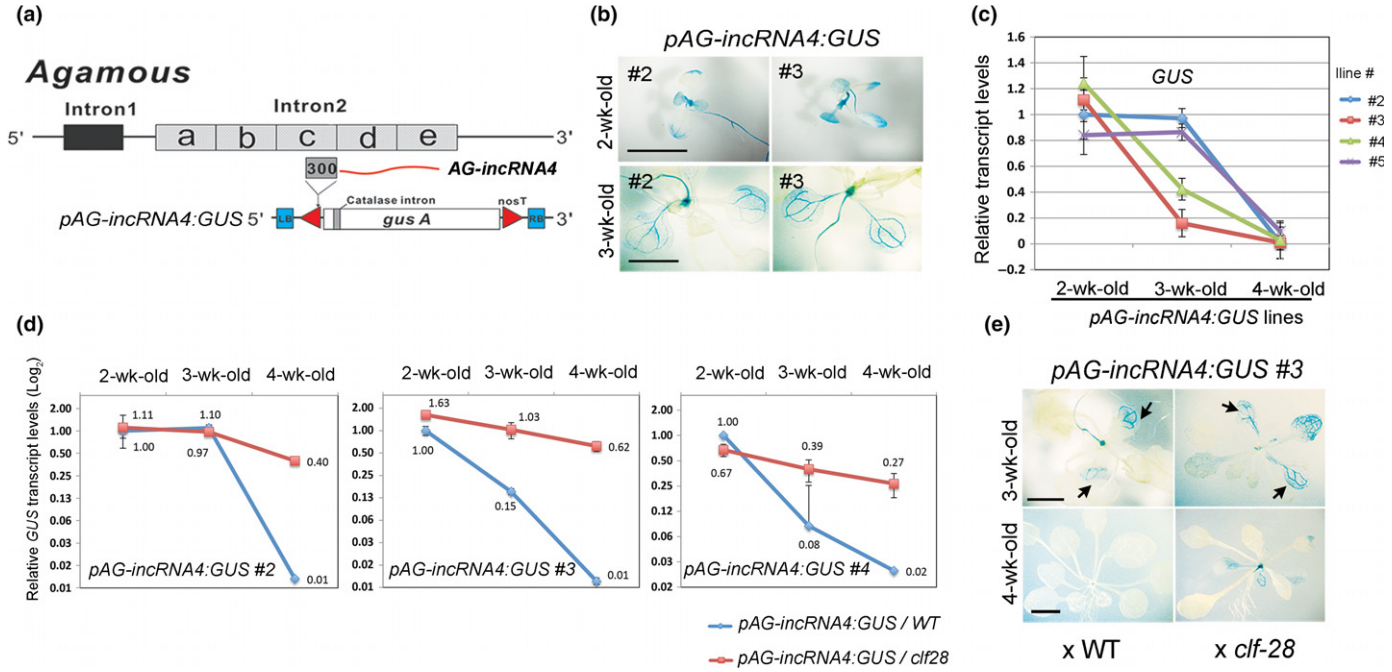

Fig. 8 Putative promoter for *AGAMOUS* (*AG*)-*incRNA4* activates tissue-specific β-Glucuronidase (GUS) expression in transgenic lines (inc, introgenic noncoding). (a) Schematic diagram of putative *AG-incRNA4* promoter:*GUS* fusion gene. (b) *AG-incRNA4* promoter determines tissue-specific *GUS* expression in *pAG-incRNA4:GUS* transgenic lines. Bars: 1.0 cm (upper panels); 0.5 cm (lower panels). (c) *GUS* mRNA levels of *pAG-incRNA4:GUS* lines (lines #2, #3, #4 and #5) in seedlings of different ages (fold-change; mean± SD of quantitative reverse-transcription polymerase chain reaction (qRT-PCR); $n = 3$). The relative value of *GUS* expression level in 2-wk-old seedlings of *pAG-incRNA4:GUS* line #2 was set as 1.0. (d) *GUS* mRNA levels of *pAG-incRNA4:GUS/WT* and *pAG-incRNA4:GUS/clf-28* lines in time-course experiments (fold change; mean± SD of qRT-PCR; $n = 3$). The relative value of *GUS* expression level in 2-wk-old *pAG-incRNA4:GUS lines #2, #3* and *#4* were set as 1.0, individually. (e) Tissue-specific *GUS* expression in *pAG-incRNA4:GUS #3/WT* and *pAG-incRNA4:GUS #3/clf-28* plants. Bars, 0.5 cm. Black arrows indicate cotyledons. All experiments were performed with three independent biological replicates.

intron 2 (Fig. 7b) to trimethylate H3K27 (Fig. 4) forming repressed *AG* chromatin. Heo & Sung (2011) have previously shown that PRC2 is recruited by incRNA of *FLC*, *COLDAIR*, via interaction between CLF CXC domain and *COLDAIR*. Our results here extend this observation to another intronic RNA. The DNA region (+2616 to +3348 within *AG* intron 2) that we identified as CLF target also contains PREs which may recruit PRC2 for gene repression (Xiao *et al.*, 2017).

Auto-regulation of *AG-incRNA4*

In contrast to the case of *COLDAIR* (Heo & Sung, 2011) we found that *AG-incRNA4* highly accumulates in *clf-28* and *GUS* mRNA levels increase in *pAG-incRNA4:GUS* in *clf-28* background. These results suggest that the *incRNA4* promoter itself is downregulated by the *incRNA4*/CLF repressor. Consistent with this notion, ChIP experiments have identified one CLF binding site located within the *AG-incRNA4* promoter region (Schubert *et al.*, 2006). We also have shown here that CLF binds to the region between the *AG-incRNA4* promoter and the DNA region coding for the 5′-end RNA (Fig. 7a).

Our results here provide evidence that the sense strand of incRNA, *AG-incRNA4*, is transcribed from *AG* intron 2 and becomes associated with CLF to suppress *AG* expression in vegetative tissues by H3K27 trimethylation. Also, *AG-incRNA4* might be downregulated by CLF and itself to autoregulate its own expression. Although the regulation of *AG-incRNA4* biogenesis is not entirely clear, it appears that this incRNA might be regulated by PRC2 to maintain a lower level for CLF recruitment. A major challenge of studying sense incRNA on plants is due to the unavailability of T-DNA insertion lines. In addition, the low incRNA expression levels and the possible contamination of genomic DNA region present challenging technical hurdles to overcome. We have attempted to overcome these technical challenges and believe our results will contribute to a better understanding of tissue-specific gene regulation in plants.

Acknowledgements

N-H.C. was funded in part by the Returning Singaporean Scientists Scheme (RSSS; NRF-RSSS-002) of the National Research Foundation, Singapore. H-W.W. received a post-doctoral fellowship (102-2917-I-564-017) from the Ministry of Science and Technology, Taiwan.

Author contributions

H-W.W. and N-H.C. designed the experiments; H-W.W, S.D., H-Z.M., H.X. and Q-W.N. performed the experiments;

© 2018 The Authors
New Phytologist © 2018 New Phytologist Trust

H.W. and J.L. analyzed the bioinformatics data; and H-W.W. and N-H.C. discussed the results and wrote the manuscript.

References

Agorio A, Vera P. 2007. ARGONAUTE4 is required for resistance to *Pseudomonas syringae* in Arabidopsis. *Plant Cell* **19**: 3778–3790.

Ariel F, Jegu T, Latrasse D, Romero-Barrios N, Christ A, Benhamed M, Crespi M. 2014. Noncoding transcription by alternative RNA polymerases dynamically regulates an auxin-driven chromatin loop. *Molecular Cell* **55**: 383–396.

Bardou F, Ariel F, Simpson CG, Romero-Barrios N, Laporte P, Balzergue S, Brown JW, Crespi M. 2014. Long noncoding RNA modulates alternative splicing regulators in Arabidopsis. *Developmental cell* **30**: 166–176.

Berger N, Dubreucq B, Roudier F, Dubos C, Lepiniec L. 2011. Transcriptional regulation of *Arabidopsis LEAFY COTYLEDON2* involves *RLE*, a *cis*-element that regulates trimethylation of histone H3 at lysine-27. *Plant Cell* **23**: 4065–4078.

Bowler C, Benvenuto G, Laflamme P, Molino D, Probst AV, Tariq M, Paszkowski J. 2004. Chromatin techniques for plant cells. *Plant Journal* **39**: 776–789.

Busch MA, Bomblies K, Weigel D. 1999. Activation of a floral homeotic gene in Arabidopsis. *Science* **285**: 585–587.

Chanvivattana Y, Bishopp A, Schubert D, Stock C, Moon YH, Sung ZR, Goodrich J. 2004. Interaction of Polycomb-group proteins controlling flowering in Arabidopsis. *Development* **131**: 5263–5276.

Cheung AY, Reddy AS. 2012. Nuclear architecture and dynamics: territories, nuclear bodies, and nucleocytoplasmic trafficking. *Plant physiology* **158**: 23–25.

Clough SJ, Bent AF. 1998. Floral dip: a simplified method for *Agrobacterium*-mediated transformation of *Arabidopsis thaliana*. *Plant Journal* **16**: 735–743.

Deyholos MK, Sieburth LE. 2000. Separable whorl-specific expression and negative regulation by enhancer elements within the AGAMOUS second intron. *Plant Cell* **12**: 1799–1810.

Ding J, Lu Q, Ouyang Y, Mao H, Zhang P, Yao J, Xu C, Li X, Xiao J, Zhang Q. 2012. A long noncoding RNA regulates photoperiod-sensitive male sterility, an essential component of hybrid rice. *Proceedings of the National Academy of Sciences, USA* **109**: 2654–2659.

Drews GN, Bowman JL, Meyerowitz EM. 1991. Negative regulation of the Arabidopsis homeotic gene AGAMOUS by the APETALA2 product. *Cell* **65**: 991–1002.

Franco-Zorrilla JM, Valli A, Todesco M, Mateos I, Puga MI, Rubio-Somoza I, Leyva A, Weigel D, Garcia JA, Paz-Ares J. 2007. Target mimicry provides a new mechanism for regulation of microRNA activity. *Nature Genetics* **39**: 1033–1037.

Goodrich J, Puangsomlee P, Martin M, Long D, Meyerowitz EM, Coupland G. 1997. A Polycomb-group gene regulates homeotic gene expression in Arabidopsis. *Nature* **386**: 44–51.

Hajdukiewicz P, Svab Z, Maliga P. 1994. The small, versatile pPZP family of Agrobacterium binary vectors for plant transformation. *Plant Molecular Biology* **25**: 989–994.

Hamaguchi A, Yamashino T, Koizumi N, Kiba T, Kojima M, Sakakibara H, Mizuno T. 2008. A small subfamily of *Arabidopsis RADIALIS-LIKE SANT/MYB* genes: a link to HOOKLESS1-mediated signal transduction during early morphogenesis. *Bioscience, Biotechnology, and Biochemistry* **72**: 2687–2696.

Henriques R, Wang H, Liu J, Boix M, Huang LF, Chua NH. 2017. The antiphasic regulatory module comprising CDF5 and its antisense RNA FLORE links the circadian clock to photoperiodic flowering. *New Phytologist* **216**: 854–867.

Heo JB, Sung S. 2011. Vernalization-mediated epigenetic silencing by a long intronic noncoding RNA. *Science* **331**: 76–79.

Karapetyan AR, Buiting C, Kuiper RA, Coolen MW. 2013. Regulatory roles for long ncRNA and mRNA. *Cancers* **5**: 462–490.

Karimi M, Inze D, Depicker A. 2002. GATEWAY vectors for Agrobacterium-mediated plant transformation. *Trends in Plant Science* **7**: 193–195.

Kim DH, Sung S. 2017. Vernalization-triggered intragenic chromatin loop formation by long noncoding RNAs. *Developmental Cell* **40**: 302–312. e304.

Liu F, Marquardt S, Lister C, Swiezewski S, Dean C. 2010. Targeted 3′ processing of antisense transcripts triggers Arabidopsis FLC chromatin silencing. *Science* **327**: 94–97.

Liu J, Deng S, Wang H, Ye J, Wu HW, Sun HX, Chua NH. 2016. CURLY LEAF regulates gene sets coordinating seed size and lipid biosynthesis. *Plant physiology* **171**: 424–436.

Liu J, Jung C, Xu J, Wang H, Deng S, Bernad L, Arenas-Huertero C, Chua NH. 2012. Genome-wide analysis uncovers regulation of long intergenic noncoding RNAs in Arabidopsis. *Plant Cell* **24**: 4333–4345.

Liu J, Wang H, Chua N-H. 2015. Long noncoding RNA transcriptome of plants. *Plant Biotechnology Journal* **13**: 319–328.

Liu X, Kim YJ, Muller R, Yumul RE, Liu C, Pan Y, Cao X, Goodrich J, Chen X. 2011. *AGAMOUS* terminates floral stem cell maintenance in *Arabidopsis* by directly repressing *WUSCHEL* through recruitment of Polycomb Group proteins. *Plant Cell* **23**: 3654–3670.

Lodha M, Marco CF, Timmermans MC. 2013. The ASYMMETRIC LEAVES complex maintains repression of KNOX homeobox genes via direct recruitment of Polycomb-repressive complex2. *Genes & Development* **27**: 596–601.

Lohmann JU, Hong RL, Hobe M, Busch MA, Parcy F, Simon R, Weigel D. 2001. A molecular link between stem cell regulation and floral patterning in Arabidopsis. *Cell* **105**: 793–803.

Mizukami Y, Ma H. 1992. Ectopic expression of the floral homeotic gene *AGAMOUS* in transgenic Arabidopsis plants alters floral organ identity. *Cell* **71**: 119–131.

Molitor A, Shen WH. 2013. The polycomb complex PRC1: composition and function in plants. *Journal of Genetics and Genomics = Yi chuan xue bao* **40**: 231–238.

Murashige T, Skoog F. 1962. A revised medium for rapid growth and bio assays with tobacco tissue cultures. *Physiologia plantarum* **15**: 473–497.

Riechmann JL, Krizek BA, Meyerowitz EM. 1996. Dimerization specificity of Arabidopsis MADS domain homeotic proteins APETALA1, APETALA3, PISTILLATA, and AGAMOUS. *Proceedings of the National Academy of Sciences, USA* **93**: 4793–4798.

Schatlowski N, Creasey K, Goodrich J, Schubert D. 2008. Keeping plants in shape: polycomb-group genes and histone methylation. *Seminars in Cell & Developmental Biology* **19**: 547–553.

Schubert D, Primavesi L, Bishopp A, Roberts G, Doonan J, Jenuwein T, Goodrich J. 2006. Silencing by plant Polycomb-group genes requires dispersed trimethylation of histone H3 at lysine 27. *EMBO Journal* **25**: 4638–4649.

Senecoff JF, McKinney EC, Meagher RB. 1996. *De novo* purine synthesis in *Arabidopsis thaliana*. II. The PUR7 gene encoding 5′-phosphoribosyl-4-(N-succinocarboxamide)-5-aminoimidazole synthetase is expressed in rapidly dividing tissues. *Plant Physiology* **112**: 905–917.

Seo JS, Sun HX, Park BS, Huang CH, Yeh SD, Jung C, Chua NH. 2017. ELF18-INDUCED LONG NONCODING RNA associates with Mediator to enhance expression of innate immune response genes in Arabidopsis. *Plant Cell* **29**: 1024–1038.

Shibuya K, Fukushima S, Takatsuji H. 2009. RNA-directed DNA methylation induces transcriptional activation in plants. *Proceedings of the National Academy of Sciences* **106**: 1660–1665.

Sieburth LE, Meyerowitz EM. 1997. Molecular dissection of the AGAMOUS control region shows that *cis* elements for spatial regulation are located intragenically. *Plant Cell* **9**: 355–365.

Singer SD, Cox KD, Liu Z. 2010. Both the constitutive cauliflower mosaic virus 35S and tissue-specific AGAMOUS enhancers activate transcription autonomously in *Arabidopsis thaliana*. *Plant Molecular Biology* **74**: 293–305.

Sun Q, Csorba T, Skourti-Stathaki K, Proudfoot NJ, Dean C. 2013. R-loop stabilization represses antisense transcription at the Arabidopsis FLC locus. *Science* **340**: 619–621.

Wang H, Chung PJ, Liu J, Jang IC, Kean MJ, Xu J, Chua NH. 2014a. Genome-wide identification of long noncoding natural antisense transcripts and their responses to light in Arabidopsis. *Genome research* **24**: 444–453.

Wang H, Niu QW, Wu HW, Liu J, Ye J, Yu N, Chua NH. 2015. Analysis of non-coding transcriptome in rice and maize uncovers roles of conserved lncRNAs associated with agriculture traits. *Plant Journal* **84**: 404–416.

© 2018 The Authors
New Phytologist © 2018 New Phytologist Trust

Wang Y, Fan X, Lin F, He G, Terzaghi W, Zhu D, Deng XW. 2014b. Arabidopsis noncoding RNA mediates control of photomorphogenesis by red light. *Proceedings of the National Academy of Sciences, USA* **111**: 10359–10364.

Whitcomb SJ, Basu A, Allis CD, Bernstein E. 2007. Polycomb Group proteins: an evolutionary perspective. *Trends in Genetics : TIG* **23**: 494–502.

Xiao J, Jin R, Yu X, Shen M, Wagner JD, Pai A, Song C, Zhuang M, Klasfeld S, He C *et al.* 2017. *Cis* and *trans* determinants of epigenetic silencing by Polycomb repressive complex 2 in *Arabidopsis*. *Nature Genetics* **49**: 1546–1552.

Yamada M. 2017. Functions of long intergenic non-coding (linc) RNAs in plants. *Journal of Plant Research* **130**: 67–73.

Zhang X, Henriques R, Lin SS, Niu QW, Chua NH. 2006. Agrobacterium-mediated transformation of *Arabidopsis thaliana* using the floral dip method. *Nature Protocols* **1**: 641–646.

Supporting Information

Additional supporting information may be found online in the Supporting Information section at the end of the article

Fig. S1 Identification of *AG-incRNAs* (*1-4*) from the first and second introns of *AGAMOUS* (*AG*).

Fig. S2 Confirmation of putative AG-incRNA4 transcript by RT-PCR.

Fig. S3 Small RNA-seq analysis of different AG-incRNAi lines (In2d/e and In2e).

Fig. S4 Analysis of DNA methylation status on *AG* Intron 2 region using bisulfite-treated DNA for PCR.

Table S1 Primer pairs used for various constructs

Table S2 Primer pairs used for real-time qPCR and 5′/3′ RACE

Table S3 Plant materials in this study

Table S4 Primer pairs used for *in vitro* transcription of RNA

Method S1 Detail of RNA sample preparation without contamination of genomic DNAs in this study.

Please note: Wiley Blackwell are not responsible for the content or functionality of any Supporting Information supplied by the authors. Any queries (other than missing material) should be directed to the *New Phytologist* Central Office.



About *New Phytologist*

- *New Phytologist* is an electronic (online-only) journal owned by the New Phytologist Trust, a **not-for-profit organization** dedicated to the promotion of plant science, facilitating projects from symposia to free access for our Tansley reviews and Tansley insights.
- Regular papers, Letters, Research reviews, Rapid reports and both Modelling/Theory and Methods papers are encouraged. We are committed to rapid processing, from online submission through to publication 'as ready' via *Early View* – our average time to decision is <26 days. There are **no page or colour charges** and a PDF version will be provided for each article.
- The journal is available online at Wiley Online Library. Visit **www.newphytologist.com** to search the articles and register for table of contents email alerts.
- If you have any questions, do get in touch with Central Office (np-centraloffice@lancaster.ac.uk) or, if it is more convenient, our USA Office (np-usaoffice@lancaster.ac.uk)
- For submission instructions, subscription and all the latest information visit **www.newphytologist.com**

© 2018 The Authors
New Phytologist © 2018 New Phytologist Trust